AN IMPROVED TARGET METHOD TO QUANTITATIVELY MEASURE THE LATERAL RESOLUTION OF THE CONFOCAL RAMAN MICROSCOPE

Xiang Ding*, Yanxhe Fu, Fei Li, Jiyan Zhang, Wenli Liu

National Institute of Metrology,
Beijing 100029, China; e-mail: dingxiang@nim.ac.cn

The lateral resolution is one of the most important hallmarks for evaluating the imaging performance of a confocal Raman microscope (CRM). A method based on the resolution test chart for testing the lateral resolution of the CRM was proposed. The test imaging target comprised a polished silicon substrate coated with a thin metallic pattern, which provided a high contrast and negligible edge effects. By using a single-bar target instead of a conventional three-bar target, quantitative measurements of the lateral resolution of the CRM were possible. Single-bar targets with different widths were used to test a CRM with a nominal lateral resolution of approximately 1 μm. The response of the CRM to the single-bar target was studied further with a theoretical model, and the relationship between the Michelson contrast of the response function and the lateral resolution was investigated. Finally, the method used to calculate the lateral resolution was described and tested and shown to have a relative repeatability of only 5.6%, which is ideal for resolution testing. Overall, our experimental results showed excellent agreement with simulation results and proved that the single-bar target method was capable of measuring the lateral resolution of CRMs with high accuracy, efficiency and reproducibility.

Keywords: *Raman imaging, lateral resolution, testing target, Fermi function, contrast.*

МЕТОД КОЛИЧЕСТВЕННОГО ИЗМЕРЕНИЯ ЛАТЕРАЛЬНОГО РАЗРЕШЕНИЯ КОНФОКАЛЬНОГО КР-МИКРОСКОПА

X. Ding*, Y. Fu, F. Li, J. Zhang, W. Liu

УДК 535.375.5:535.822

Национальный институт метрологии,
Пекин 100029, Китай; e-mail: dingxiang@nim.ac.cn

(Поступила 2 октября 2019)

Предложен метод проверки латерального разрешения конфокального КР-микроскопа (CRM) на основе калибровочной таблицы разрешения. Мишень для тестового изображения состояла из полированной кремниевой подложки, покрытой тонким металлическим рисунком, который обеспечивал высокий контраст и незначительные краевые эффекты. Использование мишени с одним стержнем вместо обычной мишени с тремя стержнями позволило количественно измерить латеральное разрешение CRM. Одностержневые мишени различной ширины использовались для тестирования CRM с номинальным поперечным разрешением ~1 мкм. С помощью теоретической модели изучен отклик CRM на мишень из одного стержня и исследована взаимосвязь между контрастом Майкельсона функции отклика и латеральным разрешением. Предлагаемый метод проверки латерального разрешения имеет относительную повторяемость 5.6 %, что идеально для контроля разрешения. Экспериментальные результаты демонстрируют отличное согласие с результатами моделирования и подтверждают, что метод одностержневой мишени позволяет измерять латеральное разрешение CRM с высокой точностью, эффективностью и воспроизводимостью.

Ключевые слова: *КР-визуализация, латеральное разрешение, контрольная цель, функция Ферми, контраст.*

Introduction. Confocal Raman microscopy (CRM) is a powerful instrument used in a wide range of fields such as archeology, chemistry, geology, criminal investigation, and pharmacy [1–4]. CRM combines Raman spectroscopy with confocal laser scanning microscopy to enable the acquisition of Raman spectra and their spatial distribution within a sample simultaneously. The spatial resolution, especially the lateral resolution, is one of the most important parameters for evaluating the instrumental performance. It is determined by both instrumental configurations and characteristics of the sample, such as thickness, opacity, and homogeneity [5].

Wilhelm et al. [6], Everall et al. [7], and Batchelder et al. [8] presented contrasting theoretical models for estimating the spatial resolution of CRMs. However, the real resolution of CRM is always worse than what is predicted theoretically due to the influence of the spectrum collecting system and the photon scattering effect [9]. Therefore, an experimentally-determined lateral resolution is the most accurate and useful. Point spread function (PSF) and line spread function (LSF) methods are used to measure the spatial resolution of optical systems by imaging either a microsphere or a line, respectively [10, 11]. However, since the feature size must be less than 1/6 of the theoretical resolution, these methods are limited [12]. Additionally, the sample is often embedded in a matrix or on the interface between the air and an substrate, which deviates from optimal imaging conditions and introduces further error [7]. More importantly, the intensity of Raman signal of the object decreases dramatically with a decreasing object size, leading to low signal-to-noise ratio (SNR) and resolution estimates with high error. The edge spread function (ESF) can be obtained by scanning across a knife edge [13], but due to the Raman enhancement effect at edges, the ESF curve of the CRM becomes seriously distorted, leading to unreliable resolution estimates [14].

The resolution test chart provides a universal method for the evaluation of the resolution of microscopes through visual observation [15]. Conventionally, the testing targets provide a qualitative assessment of resolution due to the lack of comparative data obtained. However, in modern microscopic systems, the use of CCD cameras for capturing digital micrographs opens the possibility of quantitative resolution measurements.

A novel testing target method for evaluating the lateral resolution of CRM was proposed and tested. Bar patterns with different widths were designed and used as testing target for Raman imaging. Testing targets consist of a polished silicon substrate coated with a thin, patterned layer of metal; which provided optimal imaging contrast and negligible edge effects. Using the designed, optimized testing targets, a simplified, single-bar method for quantitative lateral resolution measurements was then developed. The SNR of the response function was much higher than values obtained using the three-bar LSF method, where the bar widths must be much smaller than the resolution. A theoretical model was established to characterize the response of CRM to bar targets, and the relationship between the contrast of the response function to bar targets, and the lateral resolution was investigated with both experiments and simulations. The testing targets and methods were then validated by testing the lateral resolution of a commercial CRM. Finally, the experimental results and the measurement error were assessed.

Theory. The 1951 USAF resolution test chart is widely used to analyze the lateral resolution of imaging systems (Fig. 1a). An approximate value of the resolution is obtained by visual observation. Testing targets for optical microscopes are usually made using etching techniques to form groove patterns with sharp edges. These are unsuitable for Raman imaging systems as the Raman enhancement effect at sharp edges causes distortion during imaging and, in turn, inaccurate evaluations of resolution. In this paper, optimized Raman imaging testing target are prepared by coating a thin layer of metal pattern onto a polished silicon wafer. The metal layer is approximately 50 nm thick, which is thick enough to block the Raman signal from the underlying silicon. For Raman imaging, it provides a pattern with virtual edges that do not exhibit any deleterious edge effects, and provides maximum contrast.

Although the typical three-bar target is useful for analyzing resolution qualitatively, signals from bars in a single set interfere with each other, severely reducing the measurement accuracy. In order to enhance the accuracy sufficiently for quantitative analysis, a simplified single-bar target was developed (Fig. 1b).

The width of the bar must be much smaller than the resolution of the microscope to avoid systematic error in the LSF method [16]. For a bar with a certain width, it is the combination of two sharp edges, and therefore the response function of the bar target is equal to the sum of two ESFs (Fig. 2).

The Fermi function has an approximate shape of a typical ESF, which is differentiable and often used to fit the knife-edge curve [13]. It is expressed as

$$F(x) = \frac{a}{\exp((x-b)/c)+1} + d\,, \tag{1}$$

where x is the coordinate, and a, b, c, d are shape and position parameters of the Fermi function. The response function $I(x)$ of a bar target is expressed as

$$I(x) = \frac{1}{\exp(x/c)+1} + \frac{1}{\exp((x-t)/c)+1}, \tag{2}$$

where t is the width of the target pattern.

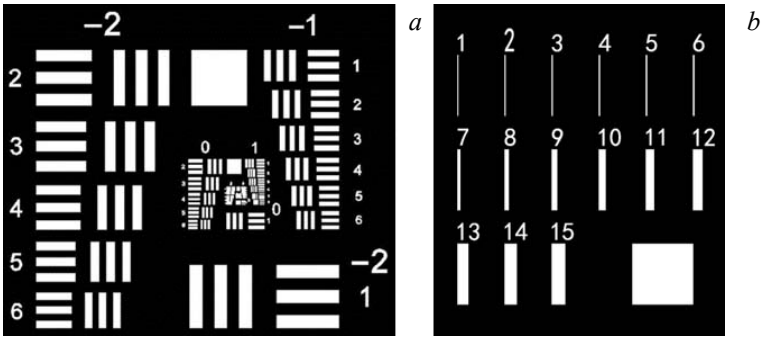

Fig. 1. The design of (a) the three-bar target and (b) the single-bar target.

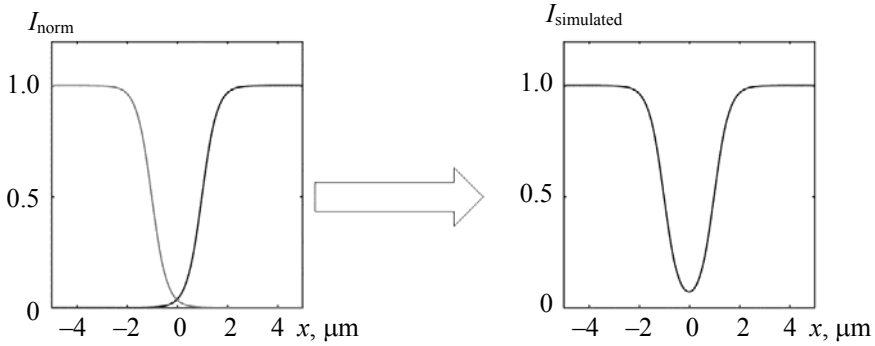

Fig. 2. The response function of a single-bar target.

The Michelson contrast is a widely used criterion to the resolving power of optical systems, which is expressed as

$$\text{contrast} = \left(I_{\max} - I_{\min}\right) / \left(I_{\max} + I_{\min}\right), \tag{3}$$

where $I_{\max}$ and $I_{\min}$ are the maximum value and the minimum value of the response function. The relationship between the contrast and the bar width is described by

$$\text{contrast} = \frac{\exp\left((t/2c)-1\right)}{\exp\left(t/2c\right)+3}. \tag{4}$$

If the Fermi function is used to fit the ESF curve, the LSF can be calculated as

$$\text{LSF} = \left|dF(x)/dx\right| = \frac{a\exp\left(-(x-b)/c\right)}{c\left(\exp\left(-(x-b)/c\right)+1\right)^2}. \tag{5}$$

The lateral resolution (LR) can be represented by the full width at half maximum (FWHM) of the LSF, which can be derived from Eq. (5):

$$\text{LR} = -2\ln\left(3-2\sqrt{2}\right)c. \tag{6}$$

An expression for the relationship between the resolution, the bar width, and the Michelson contrast, Eq. (7), can be formed by substituting Eq. (4) into Eq. (6):

$$\text{LR} = -2\ln\left(3-2\sqrt{2}\right)\frac{t}{2\ln\dfrac{1+3\text{contrast}}{1-\text{contrast}}}. \tag{7}$$

Theoretically, Eq. (7) can be used to evaluate the resolution based on sample contrast, as opposed to bar width, provided the contrast is smaller than 1. The bar width does not need to be much smaller than the resolution, as required for the LSF method. Therefore, the testing target preparation is easier and the SNR of the response function is higher.

Simulation. The CRM imaging process was simulated using the transfer function theory. When a single-bar target is imaged by the CRM, the image function $g(x,y)$ is the convolution of the top-hat function $\Pi(x,y)$ and the PSF $h(x,y)$ of the CRM:

$$g(x,y) = \Pi(x,y) \otimes h(x,y). \tag{8}$$

The Gaussian function was used to characterize the PSF of the CRM (Fig. 3). It is often used to model PSFs as it represents the common light distribution of the laser beam and numerous other independent factors. In our simulation, the FWHM of the Gaussian function was set at 1 μm.

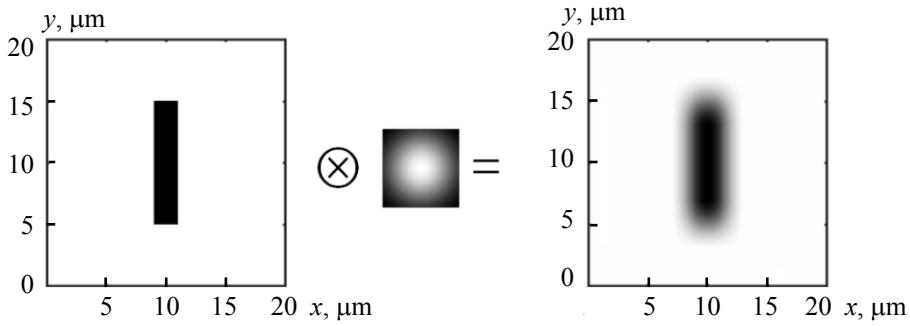

Fig. 3. The imaging process of a single-bar target.

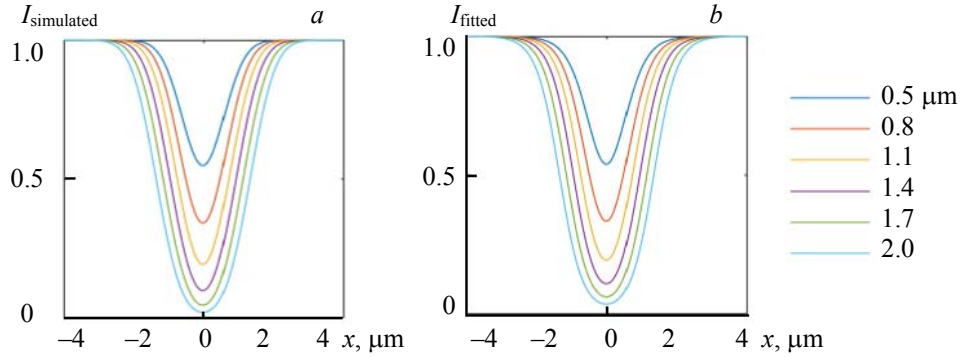

Fig. 4. Simulated results of single-bar targets with different width. (a) The response function curves; (b) the fitted results of the response function curve.

Simulations of response function curves were then performed (Fig. 4). The response function was calculated along the x direction of single-bar targets of widths 0.5 to 2 μm (Fig. 4a), then the response functions were fit with Fermi functions as defined in Eq. (2) (Fig. 4b). The R-squared of all fitted curves were higher than 99%. The relationship between the bar width and the contrasts was determined for both original experimental data and simulations, and showed that the error of contrast between the original image function and the fitted results was less than 5% (Fig. 5a). This showed that the function defined in Eq. (2) can be applied to fit the image function to yield reliable contrast and bar width data.

Finally, the relationship between the bar width and the lateral resolution calculated from fitted functions using Eq. (7) was examined (Fig. 5b). At a theoretical resolution of 1 μm, the error between calculated and theoretical values was less than 15%, which suggested that the methodology was satisfactory for real resolution measurements.

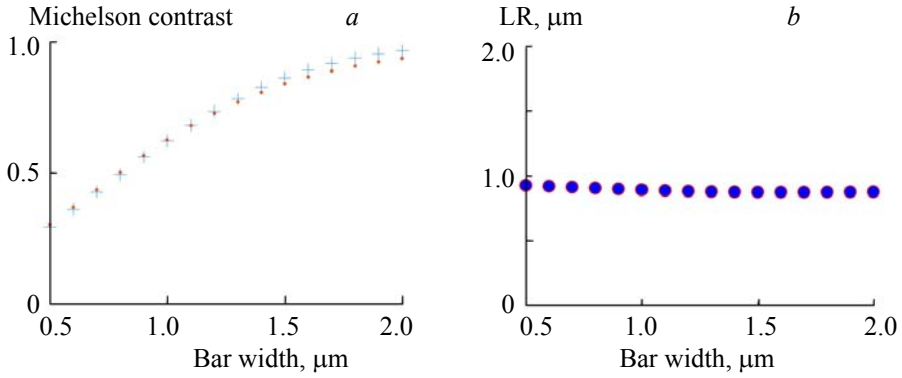

Fig. 5. (a) The relationship between the target size and the Michelson contrast, the contrast calculated from the original results (+) and from the fitted functions (•), (b) the relationship between the bar width and the LR calculated from the fitted functions.

Experiments and results. *The testing target and the instrumentation.* The testing target was prepared by depositing a thin layer (~50 nm) of chromium pattern of different widths onto a polished monocrystalline silicon substrate. Both three-bar patterns (Fig. 1a) and single-bar patterns (Fig. 1b) were prepared and tested. The three-bar target was designed according to the 1951 USAF resolution test chart, with bar widths ranging from 0.5 to 4 μm. Silicon exhibits a strong Raman peak around 520 cm^{-1}, but the chromium layer was shown to completely block the stimulating laser, and thus prevent any Raman signal originating from the underlying silicon substrate.

The testing target was imaged with a commercial CRM (Renishaw inVia) with a lateral resolution of approximately 1 μm. The stimulation laser had a wavelength of 532 nm. The magnification factor of the microscopic objective was 100×, and the numerical aperture was 0.85. The grating in the spectrometer was 2400 l/mm. The environmental temperature was 20 ± 1°C.

Experimental results. *Experiments with the three-bar target.* The three-bar targets were imaged with the CRM, where the intensity of the Raman peak of the silicon was normalized and used to calculate the gray value of the Raman image. Data obtained from bar patterns with widths 0.5, 1, 2, and 3 μm showed that the contrast increased as the bar width increased (Fig. 6). According to the principles of the 1951 USAF resolution test chart, the lateral resolution is defined by line pair per millimeter (lp/mm). The bar width of 0.5 μm corresponds to 1000 lp/mm, which represent a line pair of 1 μm. The patterns with widths of 1, 2, and 3 μm were resolved easily and clearly, while the pattern with a width of 0.5 μm could only just be resolved. The lateral resolution of the CRM was therefore shown to be approximately 1 μm. The results indicated that a three-bar target based on metal layer pattern on the silicon substrate can be used to analyze the lateral resolution of the CRM. Although the three-bar target method is intuitive and easy to use, accurate quantification of the lateral resolution is difficult. Furthermore, the difficulty in fabricating the targets increases dramatically as the bar width decreases.

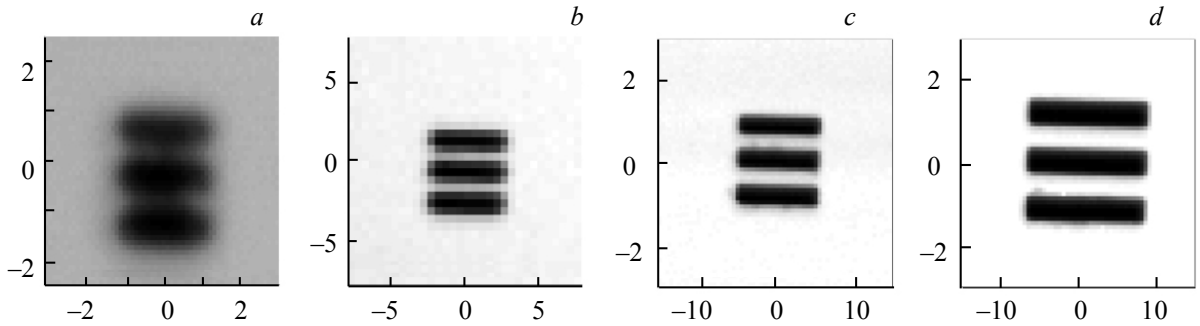

Fig. 6. The Raman image of the three-bar targets. a) 0.5, b) 1, c) 2, and d) 3 μm.

Experiments with the single-bar target. The single-bar target was scanned by the CRM in the perpendicular direction to the long edge of the pattern, and the normalized Raman intensity profiles of the silicon peak at 520 cm^{-1} were plotted in both *x* and *y* (Fig. 7) directions. The modelled curves showed a satisfactory fit with raw data, which suggested that the Fermi function, as defined in Eq. (2), was suitable for characterizing the response function of the CRM to a bar target. The lateral resolution as calculated from the response functions was then compared to bar targets with different widths (Fig. 8). The determined lateral resolution measurements were consistent across the whole range of bar widths, as predicted by theoretical simulation. The lateral resolution varied from 0.68 to 0.77 μm, and the standard deviation of relative repeatability was only 5.6%. The results of simulations and experiments indicated that the improved, simplified method based on the single-bar target enabled the quantitative measurement of the CRM lateral resolution.

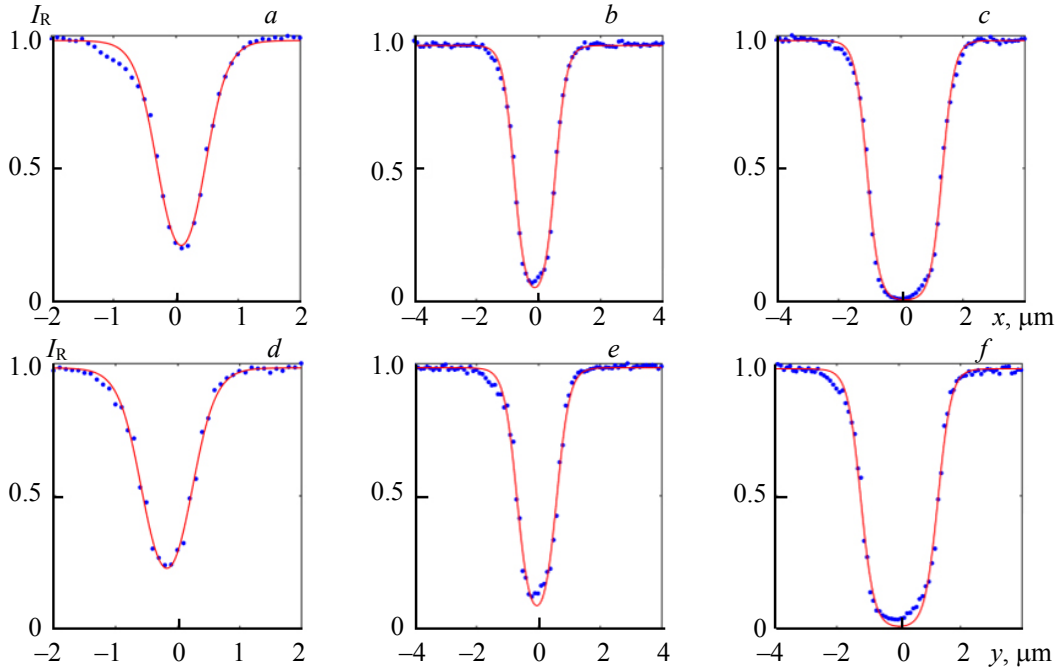

Fig. 7. The results of single-bar targets in the *x* direction. a) 0.5, b) 1, and c) 2 μm and *y* direction: d) 0.5, e) 1, and f) 2 μm.

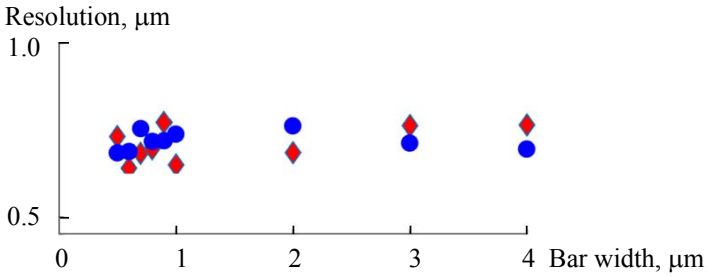

Fig. 8. The lateral resolution in the *x* direction (♦) and the *y* direction (•).

Conclusions. An improved target method for quantifying the lateral resolution of a CRM was designed, tested, and validated. The testing targets were prepared by coating a thin layered metal pattern on a polished silicon wafer substrate. Edge effects that occur from conventional groove patterns were avoided. Both three-bar targets and single-bar targets with bar widths ranging between 0.5 to 4μm were developed, used, and evaluated on a commercial CRM. The ability of the three-bar target method to evaluate the lateral resolution of the CRM was demonstrated experimentally. Although the three-bar method was easy to use, resolution measurements were qualitative and inaccurate. In contrast, the single-bar target method was used to measure the lateral resolution quantitatively and accurately. The theoretical model of the response function to single-

bar targets was established, and showed excellent agreement with experimental results. The measured lateral resolution of the CRM was between 0.68 to 0.77 μm with a standard deviation of relative repeatability of 5.6% when the bar width ranged from 0.5 to 4 μm. The combination of simulation and experimental results validated the use of the single-bar target method as an efficient, accurate, and quantitative method for the evaluation of the lateral resolution of a CRM.

Acknowledgments. The research was supported by the National Key Research and Development Program of China (2016YFF0201005).

REFERENCES

1. A. Kudelski, *Talanta*, **76**, 1 (2008).
2. P. Colomban, F. Treppoz, *J. Raman Spectrosc.*, **32**, 93 (2001).
3. P. J. Caspers, G. W. Lucassen, E. A. Carter, H. A. Bruining, G. J. Puppels, *J. Invest. Dermatol.*, **116**, 434 (2001).
4. T. J. Moore, A. S. Moody, T. D. Payne, G. M. Sarabia, A. R. Daniel, B. Sharma, *Biosensors*, **8**, 46 (2018).
5. E. Lee, B. Roussel, E. Froigneux, F. Adar, S. Mamedov, A. Whitley, *AIP Conf. Proc.*, **1267**, 166 (2010).
6. http://zeiss-campus.magnet.fsu.edu/referencelibrary/pdfs/ZeissConfocalPrinciples
7. N. J. Everall, *Analyst*; **135**, 2512 (2010).
8. D. N. Batchelder, K. J. Baldwin, *Appl. Spectrosc.*, **55**, 517 (2001).
9. J. P. Tomba, L. M. Arzondo, J. M. Pastor, *Appl. Spectrosc.*, **61**, 177 (2007).
10. R. W. Cole, T. Jinadasa, C. M. Brown, *Nat. Protoc.*, **6**, 1929 (2011).
11. F. Adar, E. Lee, S. Mamedov, A. Whitley, *Spectroscopy*, Special Issue, June01 (2006).
12. P. H. Tomlins, R. A. Ferguson, C. Hart, P. D. Woolliams, *Point-Spread Function Phantoms for Optical Coherence Tomography*, National Physical Lab. (2009).
13. A. P. Tzannes, J. M. Mooney, *Opt. Eng.*, **34**, 1808 (1995).
14. Y. Fu, X. Ding, J. Li, J. Zhang, *8th Applied Optics and Photonics China,* In press.
15. J. Li, F. Cai, Y. Dong, Z. Zhu, X. Sun, H. Zhang, S. He, *Opt. Commun.*, **392**, 1 (2017).
16. T. Jan, D. Thomas, H. Olaf, *Confocal Raman Microscopy*, Springer International Publishing, Germany, XXIV, 596 (2018).